EPJ Web of Conferences **364**, 14001 (2026) https://doi.org/10.1051/epjconf/202636414001
Quark Matter 2025

Listening to the long ringdown

A novel way to pinpoint the EOS in neutron-star cores

Christian Ecker[1,*], *Tyler* Gorda[2], *Aleksi* Kurkela[3], and *Luciano* Rezzolla[1]

[1]Institut für Theoretische Physik, Goethe Universität, Max-von-Laue-Str. 1, 60438, Germany
[2]Department of Physics, The Ohio State University, Columbus, OH 43210, USA
[3]Faculty of Science and Technology, University of Stavanger, Stavanger, 4036, Stavanger, Norway

Abstract. Gravitational waves (GWs) from binary neutron star (BNS) merger remnants complement constraints from the inspiral phase, mass–radius measurements, and microscopic theory by providing information about the neutron-star equation of state (EOS) at extreme densities. We perform general-relativistic simulations of BNS mergers using EOS models that span the uncertain high-density regime. We find a robust correlation between the ratio of energy and angular momentum lost during the late-time post-merger GW signal—the long ringdown—and the EOS at the highest densities in neutron star cores. Applying this correlation to post-merger GW signals reduces EOS uncertainty at several times saturation density, where no direct constraints currently exist.

1 Introduction

The densest matter in the observable universe resides in neutron star (NS) cores, where gravity compresses matter to densities far exceeding nuclear saturation, $n_{\rm sat} = 0.16$ baryons/fm^3. The equation of state (EOS) governing such strongly interacting matter remains uncertain, yet its precise determination could provide important insights into the phase diagram of Quantum Chromodynamics (QCD). Recent progress in constraining the EOS has come from both improved NS observations and ab-initio theory (e.g., [1]). Notably, the gravitational-wave (GW) signal from the BNS merger GW170817 revealed that tidal deformabilities of inspiralling NSs—closely linked to the EOS around 3 $n_{\rm sat}$—can be measured (e.g., [2]). Third-generation GW observatories [3, 4]. will have the sensitivity to detect post-merger signals with high SNR, providing access to densities even higher than those in the pre-merger phase. These signals exhibit spectral features that are tightly correlated with the EOS (see [5] and references therein). In recent work [6], we propose a refined approach that targets a specific late-time component of the post-merger signal—occurring between 1 and 15 ms—which we term the long ringdown. We briefly summarize this in the present proceedings contribution (for details see [6]). Analogous to black hole ringdowns, this slowly damped signal arises from a quasi-stationary, nearly axisymmetric hypermassive neutron star emitting nearly monochromatic GWs. We show that during this stage, the emitted GW energy and angular momentum follow a linear relation tied directly to the high-density EOS. Thus, observing the long ringdown at high SNR enables direct EOS constraints at the highest observable densities.

*e-mail: ecker@itp.uni-frankfurt.de

2 Methods

For the agnostic EOS construction, we use the Gaussian Process framework presented in [7]. To efficiently represent the EOS with a limited number of samples, we consider the posterior in the 4D parameter space ($M_{\rm TOV}$, $C_{\rm TOV}$, $\ln p_{\rm TOV}$, $R_{1.4}$), i.e., the mass, compactness, and central pressure of the maximally massive Tolman–Oppenheimer–Volkoff (TOV) solution, and the radius of a $1.4\,M_\odot$ star, respectively. We then perform a principal component analysis to identify a small set of EOSs that characterize the 68% credible region of the distribution. From this analysis, we select six "golden" EOSs from our ensemble: EOSs with the highest likelihood near the extrema of the 68% credible region, plus one near the origin.

We use the FUKA [8] and FIL [9] codes to simulate BNS mergers with parameters consistent with GW170817, i.e., with fixed chirp mass $\mathcal{M}_{\rm chirp} = 1.18\,M_\odot$ and three different ratios $q := M_2/M_1 = 0.7, 0.85, 1$ of the binary constituent masses M_1 and M_2. From these simulations, we extract the GW strain components (h_+,$h_\times$) and compute the slope of the emitted energy ($E_{\rm GW}$) with respect to the angular momentum ($J_{\rm GW}$), as well as the instantaneous frequency ($f_{\rm GW}$)

$$\frac{dE_{\rm GW}}{dJ_{\rm GW}} = \frac{\dot{E}_{\rm GW}}{\dot{J}_{\rm GW}} = \frac{\dot{h}_+^2 + \dot{h}_\times^2}{h_+\dot{h}_\times - \dot{h}_+ h_\times}\,, \qquad f_{\rm GW} = \frac{1}{2\pi}\frac{h_+\dot{h}_\times - \dot{h}_+ h_\times}{h_+^2 + h_\times^2}\,. \tag{1}$$

For a simple system with an $\ell = 2, m = 2$ deformation, one finds the identity $\dot{E}_{\rm GW}/\dot{J}_{\rm GW} = f_{\rm GW}/(2\pi)$, implying a linear slope during the long ringdown, where $f_{\rm GW}(t) \simeq$ const.. In practice we normalize them by their values at merger-time $\hat{E}_{\rm GW} = E_{\rm GW}/E^{\rm mer}_{\rm GW}$,$\hat{J}_{\rm GW} = J_{\rm GW}/J^{\rm mer}_{\rm GW}$.

3 Results

In Figure 1 (left panel), the thick colored lines show our selection of golden EOS models, with their corresponding ten closest neighbours in the 4D space plotted as thin lines; dots indicate the central densities reached in maximally massive stars. The black dashed lines

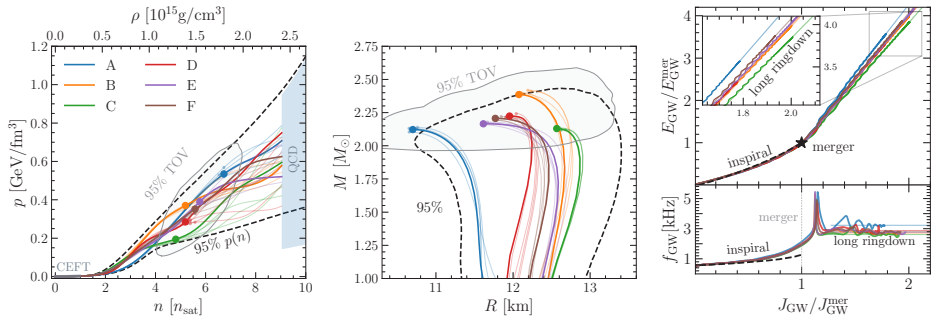

Figure 1. *Left panel:* Solid lines of different colors show the six golden EOSs (A–F) in the (p, n) plane. The dashed black lines show the 95% credible intervals of all possible EOSs, while the CEFT and QCD bounds are shown with shaded areas. Colored filled circles show the TOV points of the golden EOSs, while the solid light gray line is the 95% credible interval for all TOVs. *Middle panel:* The same as in the left but shown in the (M, R) plane. *Right panel:* Radiated GW energy and angular momentum (top), normalized to their merger values, and instantaneous GW frequency $f_{\rm GW}$ (bottom).

denote the 95% confidence interval of the entire EOS ensemble, while the blue regions indicate the imposed uncertainty bands from chiral effective field theory (CEFT) and perturbative

QCD. The middle panel presents the resulting mass–radius curves obtained by solving the TOV equations. The right panel displays one of our main results: the relation between the normalized GW energy and angular momentum (top), together with the corresponding instantaneous GW frequency (bottom), as obtained from numerical BNS merger simulations—here shown for equal-mass binaries. The key insight from these results is that $d\hat{E}_{\rm GW}/d\hat{J}_{\rm GW}$ =const. correlates with the properties of the golden EOSs.

In Fig. 2, the shaded regions show bilinear fits to the correlations between $d\hat{E}_{\rm GW}/d\hat{J}_{\rm GW}$, extracted from our simulations (symbols), and the central pressure (top) and number density (bottom) of maximally massive neutron stars (details in figure caption).

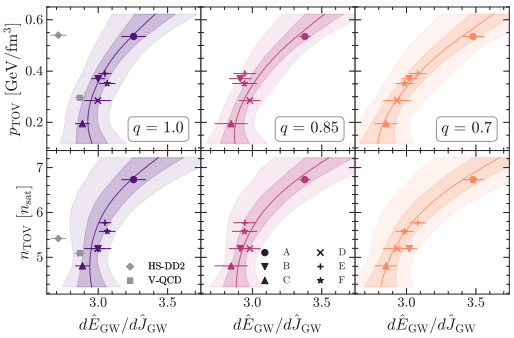

Figure 2. Data and fits of the correlations between the slope $d\hat{E}_{\rm GW}/d\hat{J}_{\rm GW}$ and $p_{\rm TOV}$ (top row) or $n_{\rm TOV}$ (bottom row), and for different mass ratios (different columns). The dark (light) shaded regions denote 68%(95%) credible intervals for the bilinear fitting model, while the solid lines denote the mean value.

These correlations in conjunction with a future post-merger GW detection, can be used to constrain the EOS at *all densities*. More specifically, we use as an additional component of the likelihood function $P(\text{data}|\text{EOS, NSs})$ the integral of our bilinear model over the measurement likelihood, in order to infer the combined EOS and NS properties via Bayes's theorem

$$P(\text{EOS, NSs}|\text{data}) = \frac{P(\text{data}|\text{EOS, NSs})P(\text{EOS, NSs})}{P(\text{data})} . \tag{2}$$

This is illustrated in Fig. 3, which presents the results of mock measurements for three different slope values and dominant post-merger frequencies f_2, assuming a ±4% measurement uncertainty. Our results show that such potential future measurements could lead to a significant reduction of the EOS uncertainty (left panel) and the corresponding mass-radius distribution of isolated neutron stars (right panel).

4 Summary

Third-generation gravitational-wave observatories will detect numerous BNS post-merger signals with high signal-to-noise ratios, enabling detailed studies of dense matter. We explore correlations between gravitational-wave observables and the equation of state (EOS) using a large set of physically consistent, generic EOSs. A principal component analysis identifies a reduced set of representative "golden" EOSs that capture the main variation in post-merger dynamics. We discover a novel correlation between the slope of the long ringdown phase—quantified by $d\hat{E}_{\rm GW}/d\hat{J}_{\rm GW}$—and the pressure and density at the maximum-mass TOV

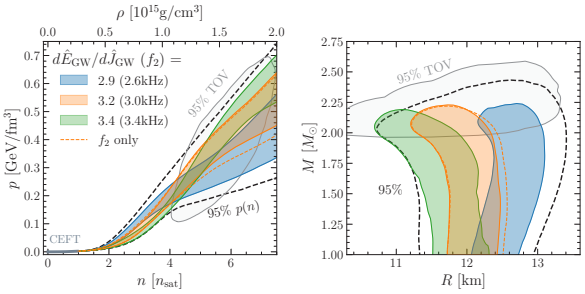

Figure 3. *Left panel* shows the 68% credibility values on the (p, n) plane from potential *joint* measurements of the slope and f_2 with ±4% uncertainty. *Right panel* the same but in the (M, R) plane.

configuration, $(p_{\rm TOV}, n_{\rm TOV})$. This slope is straightforward to extract from the waveform and provides direct constraints on the EOS at the highest core densities. By combining this correlation with Bayes' theorem, we obtain improved constraints on the mass–radius relation across the full density range, outperforming methods based solely on the post-merger peak frequency f_2.

References

[1] E. Annala, T. Gorda, J. Hirvonen, O. Komoltsev, A. Kurkela, J. Nättilä and A. Vuorinen, "Strongly interacting matter exhibits deconfined behavior in massive neutron stars," Nature Commun. **14**, no.1, 8451 (2023) https://doi.org/10.1038/s41467-023-44051-y

[2] D. Radice, S. Bernuzzi and A. Perego, "The Dynamics of Binary Neutron Star Mergers and GW170817," Ann. Rev. Nucl. Part. Sci. **70**, 95-119 (2020) https://doi.org/10.1146/annurev-nucl-013120-114541

[3] M. Evans, R. X. Adhikari, C. Afle, S. W. Ballmer, S. Biscoveanu, S. Borhanian, D. A. Brown, Y. Chen, R. Eisenstein and A. Gruson, *et al.* "A Horizon Study for Cosmic Explorer: Science, Observatories, and Community," [arXiv:2109.09882 [astro-ph.IM]]

[4] A. Abac, R. Abramo, S. Albanesi, A. Albertini, A. Agapito, M. Agathos, C. Albertus, N. Andersson, T. Andrade and I. Andreoni, *et al.* "The Science of the Einstein Telescope," [arXiv:2503.12263 [gr-qc]]

[5] G. Huez, S. Bernuzzi, M. Breschi and R. Gamba, "Kilohertz Gravitational Waves from Binary Neutron Star Mergers: Full Spectrum Analyses and High-density Constraints on Neutron Star Matter," [arXiv:2507.06293 [gr-qc]].

[6] C. Ecker, T. Gorda, A. Kurkela and L. Rezzolla, "Constraining the equation of state in neutron-star cores via the long-ringdown signal," Nature Commun. **16**, no.1, 1320 (2025) https://doi.org/10.3847/2041-8213/adef39

[7] T. Gorda, O. Komoltsev and A. Kurkela, "Ab-initio QCD Calculations Impact the Inference of the Neutron-star-matter Equation of State," Astrophys. J. **950**, no.2, 107 (2023) https://doi.org/10.3847/1538-4357/acce3a

[8] L. J. Papenfort, S. D. Tootle, P. Grandclément, E. R. Most and L. Rezzolla, "New public code for initial data of unequal-mass, spinning compact-object binaries," Phys. Rev. D **104**, no.2, 024057 (2021) https://doi.org/10.1093/mnras/stz2809

[9] E. R. Most, L. J. Papenfort and L. Rezzolla, "Beyond second-order convergence in simulations of magnetized binary neutron stars with realistic microphysics," Mon. Not. Roy. Astron. Soc. **490**, no.3, 3588-3600 (2019) https://doi.org/10.1093/mnras/stz2809